

Sn₂Sb₂S₅ films for photovoltaic applications

A. GASSOUMI*, M. KANZARI

Laboratoire de Photovoltaïque et Matériaux Semiconducteurs -ENIT BP 37, Le belvédère 1002-Tunis

In this paper we propose that Sn₂Sb₂S₅ is one of the main candidates of thin film absorbers materials. Sulfosalt Sn₂Sb₂S₅ thin films have been deposited on glass substrates by vacuum evaporation method. The pressure during evaporation was maintained at 10⁻⁵ Torr. The films were annealed in air atmosphere in the temperatures range 100-250°C. Two optical direct transitions were found. Absorption coefficients higher than 10⁴ cm⁻¹ were found. The X-ray diffraction analysis indicates that before and after annealing only the Sn₂Sb₂S₅ phase is present. Sn₂Sb₂S₅ thin films exhibit N-type conductivity after annealing. We present a model that helps to explain the evolution of photovoltaic effect.

(Received March 5, 2009; accepted April 23, 2009)

Keywords: Sn₂Sb₂S₅, Thin films, Optical properties, X-ray diffraction, Surface morphology

1. Introduction

Photovoltaic has the potential to become a major source of energy and to have a significant and beneficial effect on the global environment. Solar energy can be converted into other forms of energy, such as heat and electricity. Photovoltaic or solar cells change sunlight directly into electricity. In an effort to prepare thin films of novel semiconductor materials that contain only cost effective, abundant, and relatively less-toxic materials such as the sulfosalt thin films Pb₉Sb₈S₂₁ [1].

Studying the optical, structural and electrical properties of the sulfosalts materials has attracted great attention due to their interesting technological applications [2]. Sulfosalts belong to a class of complex sulfides with general formula of A_mB_nX_p, where A stands for metallic elements like Sn and Pb, B represents semi-metallic elements such as As, Sb, and Bi, and X can be either S or Se [3]. There are no reports after our knowledge, on the material Sn₂Sb₂S₅ in thin films form. This work deals with the effect of heat treatment in air atmosphere on structural, optical and electrical properties of the new absorber material Sn₂Sb₂S₅ in thin films form.

2. Experimental procedure

2.1. Synthesis of Sn₂Sb₂S₅

Stoichiometric amounts of 99.999% pure Sn, Sb, and S were used to prepare the initial ingot of Sn₂Sb₂S₅. The mixture was sealed in vacuum in a quartz tube. The quartz tube was heated slowly (10 °C/h). A complete homogenization could be obtained by keeping the melt at 600 °C for about 48 h. The tube was then cooled at a rate of 10 °C/h, so that cracking due to thermal expansion of the melt upon solidification was avoided. X-ray analysis of the powdered material (Fig. 1) showed that only a homogenous Sn₂Sb₂S₅ phase was present in the ingot in comparison with the reference sample [4]. A crushed

powder of this ingot was used as raw material for the thermal evaporation.

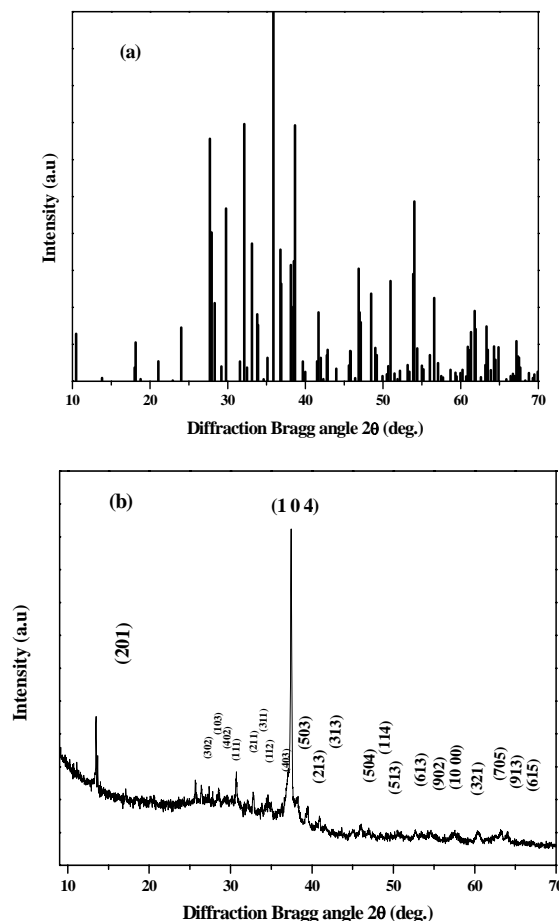


Fig.1. X-ray diffractogram of the Sn₂Sb₂S₅ powder (a): Ref [4] and (b): this work.

2.2. Film preparation

Sn₂Sb₂S₅ films were deposited on un-heated glass substrates by thermal vacuum evaporation. The pressure during the evaporation was maintained at 10⁻⁵ Torr. A chromel-alumel thermocouple monitored the substrate temperature. The as-deposited Sn₂Sb₂S₅ films were thermally annealed for 1 hour under air atmospheric in the temperature range 100-250 °C with a step of 50 °C.

2.3. Characterization of the films

The structural properties were determined by X-ray diffraction (XRD) using cobalt CoK_{α1} radiation (λ=0.1789 nm). Optical transmittance and reflectance were measured at normal incidence with a UV-visible-NIR Shimadzu 3100S spectrophotometer in the wavelength range 300–1800 nm. The film thicknesses were calculated from the positions of the interference maxima and minima in the reflectance spectra using a standard method [5]. The film thicknesses were found to be in the range 292-423 nm. The surface morphology and roughness of the films were examined means of atomic force microscopy (AFM) type Veeco model D3100 with a tapping mode and scanning electron microscopy (SEM) micrographs were performed using a Philips XL30 microscope. The hot probe method measurements were carried out in order to determine the conduction type of the samples.

3. Results and discussion

3.1. Structural and morphological properties

Fig. 2 shows the XRD patterns of the Sn₂Sb₂S₅ thin films before and after air heat treatment. As a surprising, the as-deposited Sn₂Sb₂S₅ film is crystallized in spite of the low substrate temperature (25 °C). Because in general semiconducting or dielectric materials deposited by thermal evaporation method present a dominant amorphous component the Sn₂Sb₂S₅ shows an exceptional case since it is deposited in crystalline form at low substrate temperature. Only the strong principal diffraction line related to the Sn₂Sb₂S₅ phase appeared before annealing. After annealing, the strong principal diffraction line is accompanied by a minor secondary diffraction line which is associated to the Sn₂Sb₂S₅ phase.

The crystallite size (*D*) is calculated using the well-known Scherrer's formula [6]:

$$D = \frac{0.9\lambda}{\beta \cos \theta} \quad (1)$$

where β is the value of the full width at half maximum (FWHM).

The average grain size of the layers were calculated using the principal diffraction line. The size was evaluated to be in the range (204-212) Å as shown in Fig. 3. It is clear that the heat treatment in air atmosphere does not

affect significantly the grain size of the Sn₂Sb₂S₅ thin films.

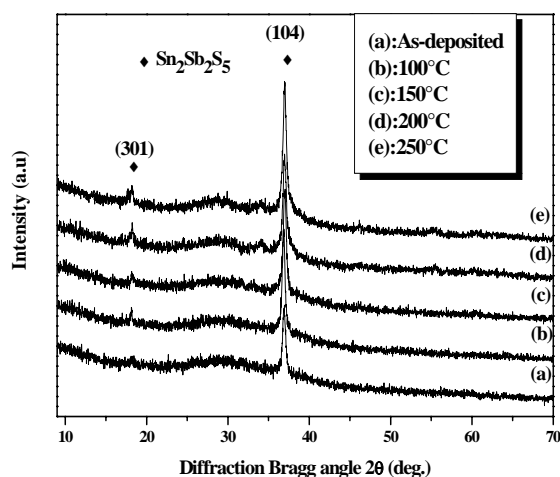


Fig. 2. X-ray diffraction patterns of as-deposited and annealed Sn₂Sb₂S₅ thin films at various annealing temperatures

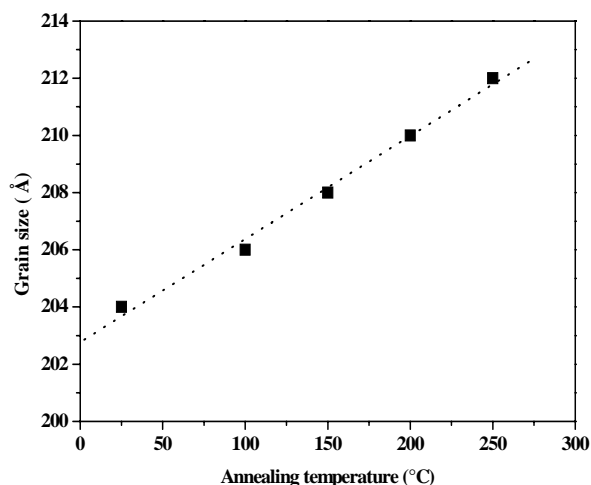


Fig.3. Grain size versus the annealing temperature of the polycrystalline Sn₂Sb₂S₅ thin films

Fig. 4 shows SEM micrographs of the as-deposited and air-annealed films at different annealing temperatures: (a) As-grown, (b) 100 °C, (c) 150 °C, (d) 200 °C, (e) 250 °C. Isolated particle growth is observed at the surfaces in particular at higher annealing temperatures. The particles were distributed homogeneously on annealed surfaces and a difference in number and size with increasing annealing temperature is observed.

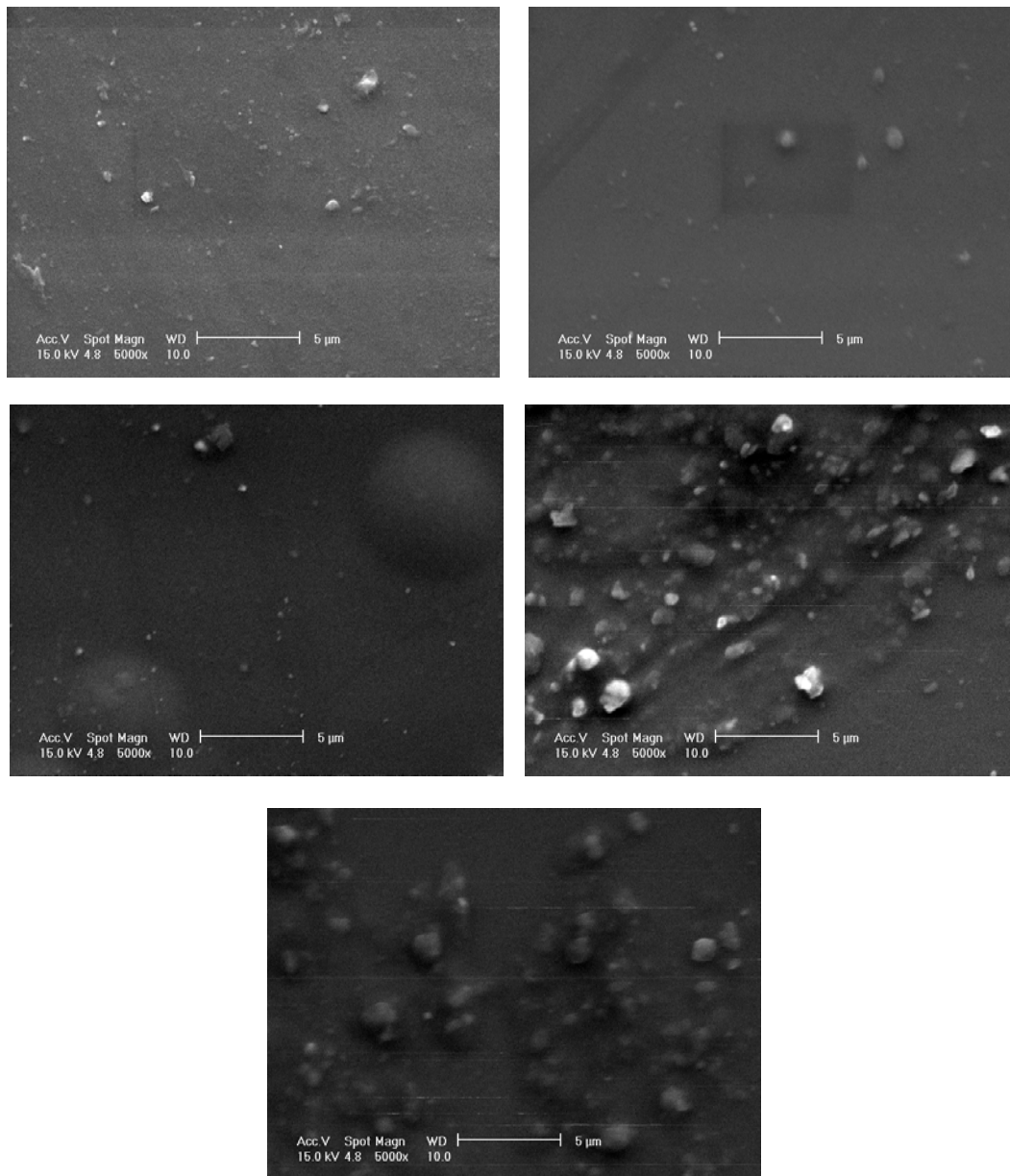


Fig. 4. Scanning electron micrographs of as-deposited and annealed $\text{Sn}_2\text{Sb}_2\text{S}_5$ thin films at temperatures: 100 °C; 150 °C ; 200°C and 250 °C.

In order to clarify the role of the thermal annealing effect, we studied surface morphologies of the $\text{Sn}_2\text{Sb}_2\text{S}_5$ films by Atomic Force Microscopy (AFM). Fig. 5 shows the surface morphologies analyzed by AFM.

It should be easily found that a low rough surface was obtained independently of the annealing temperature with average roughness of 7.6 nm. The roughness seems to be extraordinarily low, since the average thickness of the films is 350 nm.

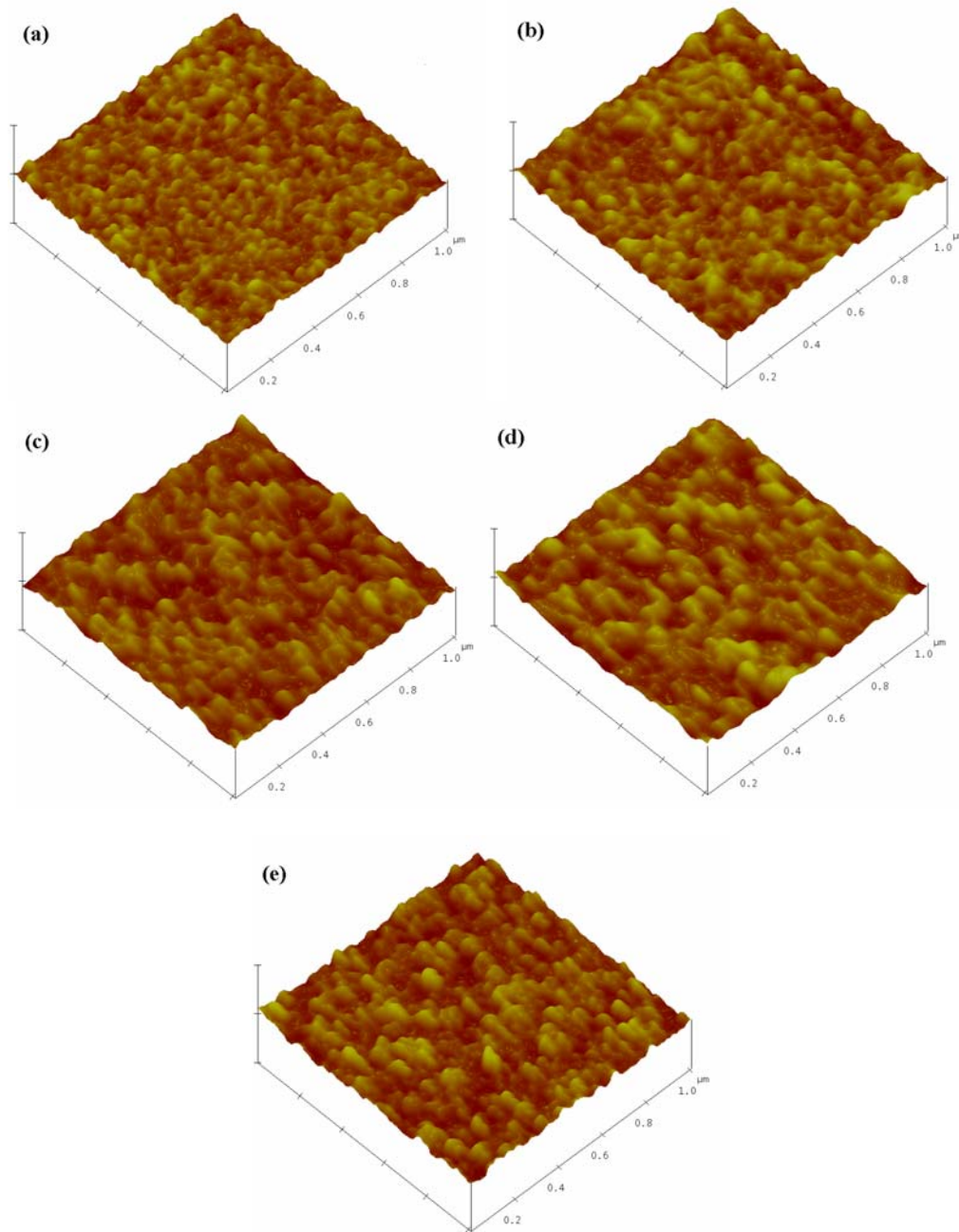


Fig.5. 3D AFM images of Sn₂Sb₂S₅ films surface: (a) As-deposited, (b) 100°C, (c) 150°C, (d) 200°C and (e) 250°C.

3.2. Optical properties

3.2.1. Optical transmittance and reflectance spectra

The optical properties of the Sn₂Sb₂S₅ thin films were studied by measuring at normal incidence both transmittance (T) and reflectance (R) spectra in the spectral range 300–1800 nm. Fig. 6 shows the transmittance and the reflectance spectra respectively

before and after annealing. All the spectra reveal very pronounced interference effects in the transparency region 900–1800 nm with sharp fall of transmittance at the band edge. The transmittance values were in the range 55–60% in the transparency region for the samples before and after air heat treatment. In addition the values of the reflectance for all the samples were in the range 40–45% which means that no absorption occurs in the spectral range 900–1800 nm.

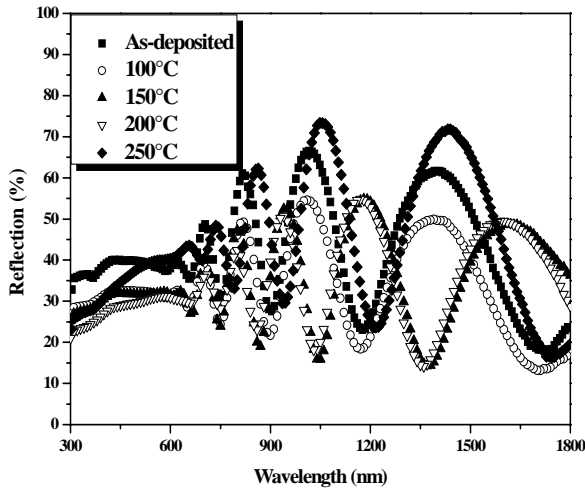
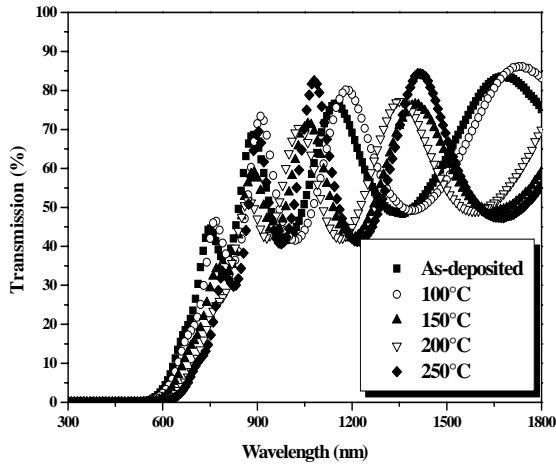


Fig.6. Transmittance (a) and reflectance (b) spectra of $Sn_2Sb_2S_5$ thin films at various annealing temperatures.

3.2.2. Values of the refractive indices

The values of the refractive indices (n) of the $Sn_2Sb_2S_5$ films were calculated approximately from the method described in [7]. Fig. 7 shows the refractive index, n , of the $Sn_2Sb_2S_5$ films as a function of wavelength for the different annealing temperatures. The refractive index increases by increasing the annealing temperature from 2.62 to 2.8. Therefore we think that antimony element is the main responsible for the increase of the refractive index by increasing the annealing temperature. Indeed, it has been shown [8, 9] that after annealing temperature materials which contain antimony compound present an opaque aspect with high refractive indices.

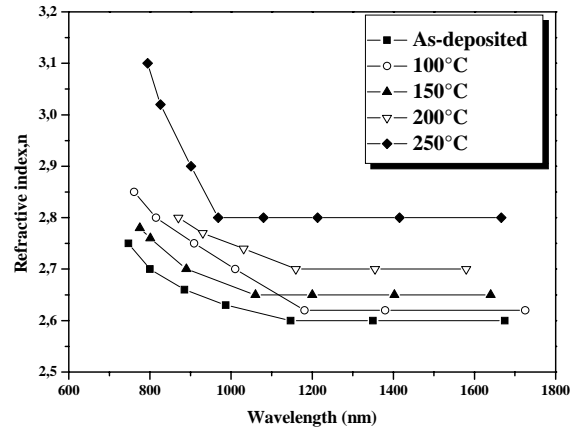


Fig.7. Refractive index n versus the wavelength for $Sn_2Sb_2S_5$ thin films at various annealing temperatures.

3.2.3. Absorption coefficients

To calculate the absorption coefficient $\alpha(h\nu)$, the following relationship was used [10]:

$$\alpha = \frac{1}{d} \ln \left[\frac{(1-R)^2}{T} \right] \quad (2)$$

where d is the film thickness, and R and T are the reflection and transmission coefficient, respectively. Fig. 8 shows the dependence of the absorption coefficient on photon energy for the $Sn_2Sb_2S_5$ films. It can be seen that all the $Sn_2Sb_2S_5$ films have relatively high absorption coefficients, higher than 10^4 cm^{-1} in the visible and the near-IR spectral region. This result is very important because the spectral dependence of the absorption coefficient is one of the important factors which affect the solar conversion efficiency.

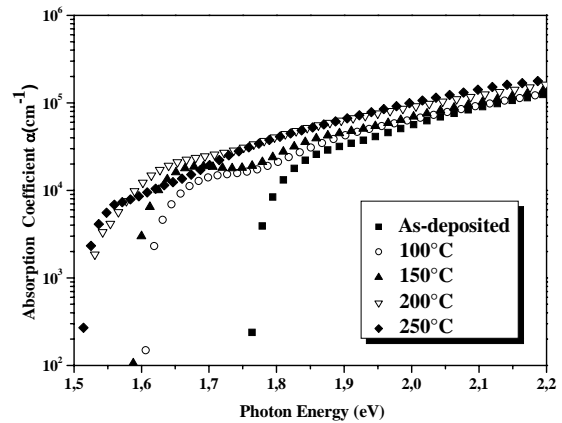


Fig.8. Absorption coefficient of the $Sn_2Sb_2S_5$ thin films for several annealing temperatures.

3.2.4. Energy gaps

The absorption coefficient α is related to the energy gap E_g according to the equation [11]:

$$\alpha h\nu = A(h\nu - E_g)^n \quad (3)$$

where A is a constant, h is the Planck constant and n is equal to $\frac{1}{2}$ for a direct gap and 2 for an indirect gap semiconductor. The band gap value E_g was determined by extrapolating the straight section of the $(\alpha h\nu)^2$ vs. $h\nu$

curve to the horizontal photon energy axis (Fig. 9). Two direct band gaps corresponding to the energy gaps E_{g1} and E_{g2} were found for each sample. The energy gaps values E_{g1} are estimated to be in the range 1.52–1.78 eV (Fig. 10) which corresponds to the valence band-conduction band transition. It was also found that E_{g1} decreases with increasing the annealing temperature. The transition with E_{g2} in the range 1.80-1.96 eV is probably associated with valence band spilling under the influence of the crystal field of lattice (Δ_{CF}) as observed in several materials [12,13].

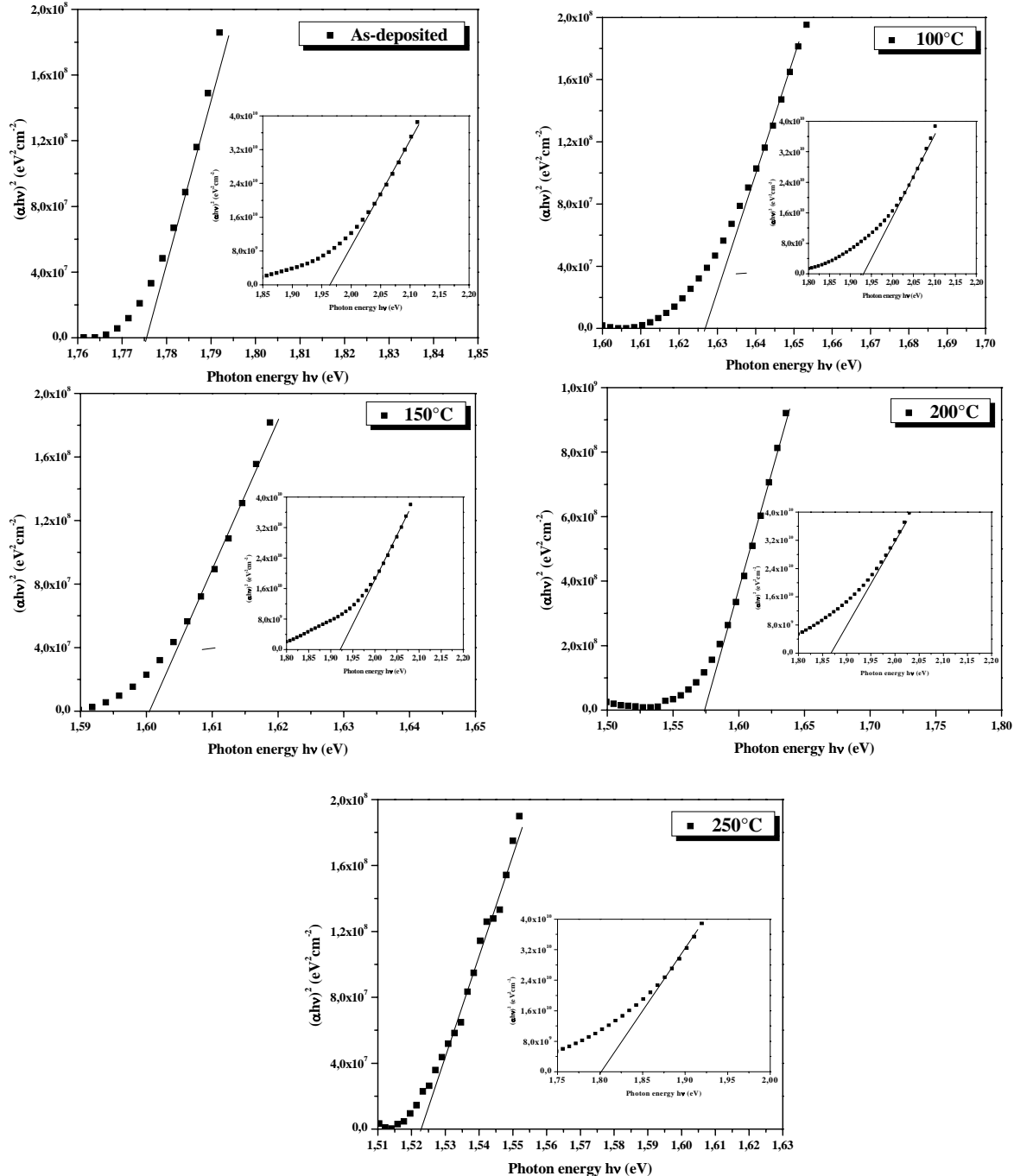


Fig.9: Plots of $(\alpha h\nu)^2$ versus $h\nu$ for the Sn₂Sb₂S₅ layers for various annealing temperatures.

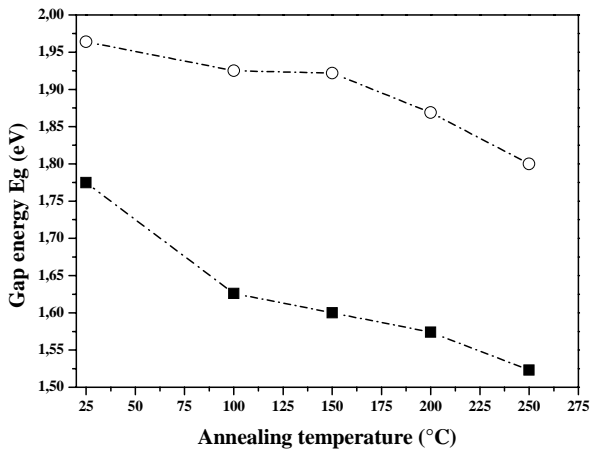


Fig.10: Band gap energies E_{g1} and E_{g2} dependence of the annealing temperature of the $\text{Sn}_2\text{Sb}_2\text{S}_5$ thin films.

3.3. Electrical properties

Besides the optical properties, the electrical properties are also an important aspect of the performance of $\text{Sn}_2\text{Sb}_2\text{S}_5$ thin films. Before annealing, the as-deposited $\text{Sn}_2\text{Sb}_2\text{S}_5$ samples are highly compensated and no significantly conduction type is observed. After annealing in air all the films presented low electrical resistivity with low N-type conductivity. The resistivity decreases after annealing at 100°C until $35 \times 10^{-4} \Omega\text{cm}$ and increases to $14 \times 10^{-3} \Omega\text{cm}$ when the films were annealed at 250°C. The origin of the N-type conductivity after air annealing is not understood at this state since no works were reported for this material in thin films forms. However we suggest that after the annealing in air a donor level is introduced and in this which can explain the origin of the N-type conductivity. In this case the effect of the oxygen incorporation is not understood since no oxide phases were detected in the samples.

4. Conclusions

This study deals with the new absorber $\text{Sn}_2\text{Sb}_2\text{S}_5$ material in thin film form. $\text{Sn}_2\text{Sb}_2\text{S}_5$ films were deposited by thermal evaporation method on glass substrates. The $\text{Sn}_2\text{Sb}_2\text{S}_5$ powder from an ingot previously synthesized by Bridgman method was used as raw material for the thermal evaporation. The as-deposited films were annealed in air atmosphere in the temperature range 50-250°C. The

as-deposited films were crystallized and no great effect on structural properties after annealing was found. Absorption coefficients higher than 10^4 cm^{-1} were found. Two optical direct transitions were found which decrease with increasing the annealing temperature. The first band gap in the range 1.52–1.78 eV is attributed to the transition valence band to conduction band. The second energy band gap in the range 1.80-1.96 eV corresponds probably to the valence band spilling under the influence of the crystal field of lattice. We found that the $\text{Sn}_2\text{Sb}_2\text{S}_5$ thin films exhibit N-type conductivity after annealing with lower resistivity.

References

- [1] Matthieu Y. Versavel, Joel A. Haber, Thin Solid Films. **515**, 5767 (2007).
- [2] H. Dittrich, A. Bieniok, U. Brendel, M. Grodzicki, D. Topa, Thin Solid Films. **515**, 5745 (2007).
- [3] G. N. Kryukovaa, M. Heuerb, G. Wagnerb, T. Doeringb, K. Bente, Journal of Solid State Chemistry. **178**, 376 (2005).
- [4] P. P. K. Smith, B. G. Hyde, Acta Crystallogr., Sec. C. **39**, 1498 (1983).
- [5] K. L. CHOPRA, Thin Film Phenomena, McGraw-Hill, New York, p. 721 (1969).
- [6] S. F. Bartram, Handbook of X-Rays, edited by E.F. Kaellebe, McGraw-Hill, New York. Chap.17 (1967).
- [7] M. Zribi, M. Kanzari, B. Rezig Materials Letters. **60**, 98 (2006).
- [8] A. Gassoumi, M. Kanzari and B. Rezig. Eur. Phys. J. Appl. Phys. **41**, 91 (2008).
- [9] A. Rabhi, M. Kanzari M, B. Rezig, Materials Letters. **62**, 3576 (2008).
- [10] M. Balkanski, T. S. Moss, Optical Properties of Semiconductors, Elsevier Science & Technology Books (1994).
- [11] E. A. Davis, N. F. Mott, Philipp. Mag. **22**, 903 (1970).
- [12] A. H. Ammar, A. M. Farid, M. A. M. Seyam, Vacuum. **66**, 27 (2002).
- [13] I. V. Bodnar, I. T. Bodnar, I. A. Victorov, V. F. Gremenok, M. Leon, Moldavian Journal of the Physical Sciences. **5**, 3 (2006).

*Corresponding author: abdelaziz.gassoumi@gmail.com